Amorphous soft-magnetic ribbons studied by ultra-small-angle polarized neutron scattering

2010 J. Phys.: Conf. Ser. 211 012027

(http://iopscience.iop.org/1742-6596/211/1/012027)

Journal of Physics: Conference Series **211** (2010) 012027 doi:10.1088/1742-6596/211/1/012027

Amorphous soft-magnetic ribbons studied by ultra-small-angle polarized neutron scattering

G Badurek[1], E Jericha[1], R Grössinger[2] and R Sato-Turtelli[2]

[1]Atominstitut, Vienna University of Technology, Stadionallee 2, A-1020 Wien, Austria
[2]Institut of Solid-State Physics, Vienna University of Technology, Wiedner Hauptstrasse 8, A-1040 Wien, Austria

E-mail: badurek@ati.ac.at

Abstract. When we investigated the magnetic structure of a variety of soft-magnetic amorphous ribbons by means of ultra-small-angle neutron scattering (USANSPOL) we were confronted with one particularly interesting $Fe_{65.7}Co_{18}Si_{0.8}B_{15.5}$ ribbon, provided by VAC Hanau. Due to a special thermal treatment during production a field- and stress-induced transverse domain texture was expected. Although the USANSPOL technique encountered its resolution limits during the investigation of this specific sample ribbon, such a texture could indeed be verified.

1. Introduction

Amorphous soft-magnetic materials represent an attractive source material for novel highly efficient magnetic shielding. Fabricated as ribbons under various heat treatment and applied stress conditions these materials may exhibit anisotropic orientation of the magnetic domains with respect to the ribbon axis. Such samples are relatively homogeneous with respect to nuclear scattering but residual material inhomogeneities may be identified by the then arising interference of nuclear and magnetic scattering contributions. Here we report on the investigation of an extremely soft-magnetic amorphous $Fe_{65.7}Co_{18}Si_{0.8}B_{15.5}$ ribbon provided by VAC Hanau, which due to its specific production conditions was expected to exhibit a field- and stress-induced transverse domain texture. According to the size ranges involved we used the novel ultra-small angle scattering technique with polarized neutrons (USANSPOL), which in combination with strong birefringent static magnetic fields exploits the extremely narrow width of Bragg reflections at perfect silicon crystals to resolve the tiny angular differences between spin-*up* spin-*down* neutrons and hence to discern magnetic from nonmagnetic scattering [1, 2, 3]. Since scattering from this sample was quite weak and partly hidden behind the resolution function, our investigations can also be understood as a demonstration of the actual capabilities of USANSPOL when it encounters its resolution limit.

2. Experimental setup

The measurements were performed at the dual purpose, so-called CRG-B instrument S18 of the Institut Laue-Langevin (ILL) in its ultra-small-angle scattering (USANS) configuration [4].

There two monolithic channel-cut perfect silicon crystals are mounted on an optical bench in non-dispersive antiparallel orientation of their (220) lattice planes (Fig. 1). Due to the narrow angular width of perfect crystal Bragg reflections scattering from the sample can be resolved with extreme angular resolution by sweeping the analyzer crystal in tiny precisely controlled rotational steps over the antiparallel orientation, thereby keeping the monochromator at a fixed angle with respect to the incident beam. Triple reflections at both the monochromator and the analyzer improve the angular resolution by causing a drastic reduction of the side wing intensity if no sample is present. To achieve optimal performance possible single-bounce particle trajectories are suppressed by cutting a vertical slit into one of the crystal plates of the analyzer that is then filled by a Cd sheet. When a monochromatic neutron beam is refracted at both

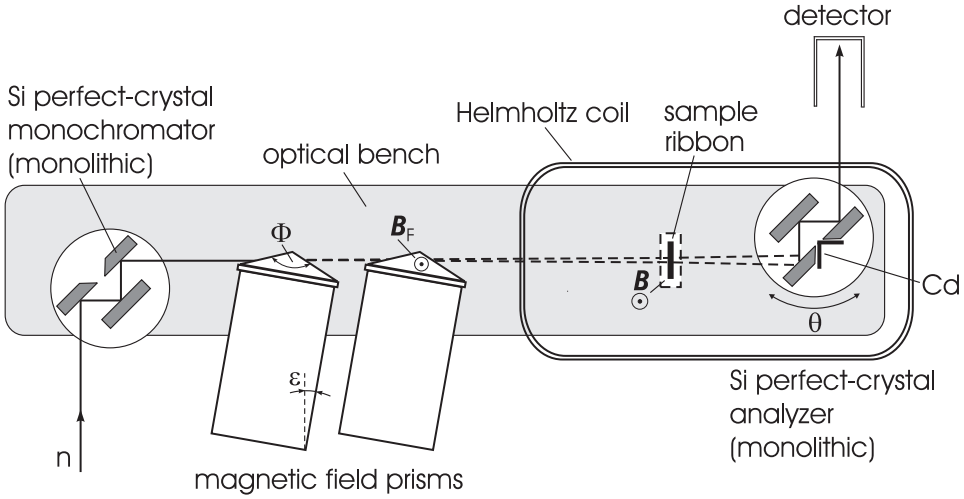

Figure 1. Schematic sketch of the experimental setup for ultra-small-angle scattering of polarized neutrons. The monochromator crystal is placed behind massive radiation shielding (not shown) in an interruption section of the thermal neutron guide H-25 of the high-flux reactor of the ILL Grenoble.

the entrance and the exit boundary of a prismatically shaped static magnetic field region the spin-*up* (↑)and spin-*down* (↓) neutrons leave this region along two different trajectories, since the field acts as a birefringent medium with an index of refraction

$$n_{\uparrow\downarrow} = 1 + \frac{\Delta k_{\uparrow\downarrow}}{k} \simeq 1 \pm \frac{m\mu B}{\hbar^2 k^2} = 1 \pm \frac{\mu B}{2E} \,. \tag{1}$$

There E is the energy, k the wave number, m the mass, and μ the magnetic moment of the neutrons. Although for thermal neutrons the angular separation of these trajectories [5]

$$\delta(E, B, \Phi, \varepsilon) = \frac{2\mu B}{E} \frac{\sin\Phi}{\cos\Phi + \cos(2\varepsilon)} \,, \tag{2}$$

where Φ is the apex angle of this 'field prism' and ε the deviation angle from symmetric passage through the prismatic field region, is typically only of the order of a few μrad, the extremely narrow resolution function $R(\theta)$ (usually called '*rocking curve*') of a USANS facility can be exploited for a clear separation of the two spin states, as illustrated in Fig. 2. This clearly twin-peaked rocking curve was obtained by means of two NdFeB-based magnet yokes, establishing a homogeneous field $B_\mathrm{p} \simeq 0.9\,\mathrm{T}$ within their prismatically shaped ($\Phi = 116°$) air gaps of 1 cm

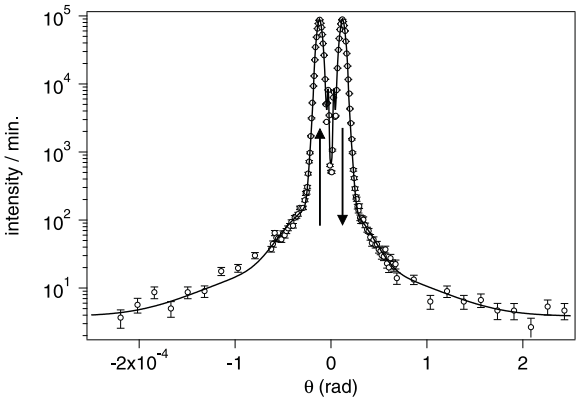

Figure 2. Rocking curve measured with empty sample holder. The arrows indicate the spin orientation with respect to the field direction. Due to the logarithmic vertical scale the peaks caused by $\lambda/2$ neutrons appear quite exaggerated. They have, however, negligible influence on the data evaluation which is restricted to the outward shoulders and wings of the measured intensity distributions.

height, at a neutron wavelength of 1.9 Åand an asymmetric passage angle $\varepsilon \simeq 25°$ (which turned out to be the maximally possible value under the conditions given). The $21.4 \pm 0.5\,\mu$m thin soft-magnetic amorphous $Fe_{65.7}Co_{18}Si_{0.8}B_{15.5}$ sample ribbon was provided by VAC, Hanau. It had a width of 25 mm and was cut to a length of 250 mm. Due to a specific thermal treatment (20 s at $T = 370°$) under simultaneously applied longitudinal tensile stress (∼50 MPa) and transverse magnetic field the ribbon was expected to exhibit some transverse magnetic anisotropy with both stress- and field-induced contributions. Hysteresis measurements provided by VAC revealed a highly linear zero remanence magnetization curve with a relative permeability H_r ∼5000, an extremely low coercive field $H_\mathrm{c} \simeq 0.01\,\mathrm{A/cm}$, a saturation induction $B_\mathrm{s} = 1.737\,\mathrm{T}$ and a magnetostriction constant $\lambda_\mathrm{s} = +4.2 \times 10^{-5}$. A dedicated sample holder allowed to orient the ribbon either horizontally or vertically. In the latter case a variable tensile stress could be applied to the otherwise freely hanging ribbon by clamping Pb weights on its bottom end. A large Helmholtz-coil surrounding both the sample region and the analyzer crystal allowed to apply a small homogeneous magnetic field to the ribbon which was sufficiently large, however, to achieve magnetic saturation. During each individual measurement this field was kept precisely at its respective preset value by means of a flux-gate sensor whose output was used to control the DC current that was fed into the coils. Disturbing influences of large magnet facilities installed in the vicinity of the instrument S18 could thus be eliminated completely.

3. Results of measurements

The differential cross-section for elastic scattering of a fully polarized incident beam can formally be written as the sum of a purely nuclear and a purely magnetic contribution and a corresponding interference term:

$$\left(\frac{\mathrm{d}\sigma}{\mathrm{d}\Omega}\right)_{\uparrow\downarrow} = F_\mathrm{n}^2 + F_\mathrm{m}^{\perp 2} \pm 2F_\mathrm{n}F_\mathrm{m}^{\perp}\,. \tag{3}$$

The subscript $^\perp$ indicates, however, that magnetic scattering is caused only by magnetization components with orthogonal orientation relative to the scattering plane. Fig. 3 shows the measured intensity distributions both for horizontal and vertical alignment of the ribbon, when the field at the sample position is set to zero as close as possible and no external mechanical stress is applied. Fig. 4 shows the analogous scattering patterns if a magnetic field of 10.9 G is applied. According to Eq. (3) the obvious lack of scattering asymmetry for the two spin states implies that there is no interference between nuclear and magnetic scattering. However, since scattering is largely reduced if the ribbon is saturated magnetically, it is of purely magnetic origin and contributions from structural or chemical inhomogeneities are negligible. Since in the case of $B = 0\,\mathrm{G}$ the measured scattering distribution is narrower for vertical than for horizontal

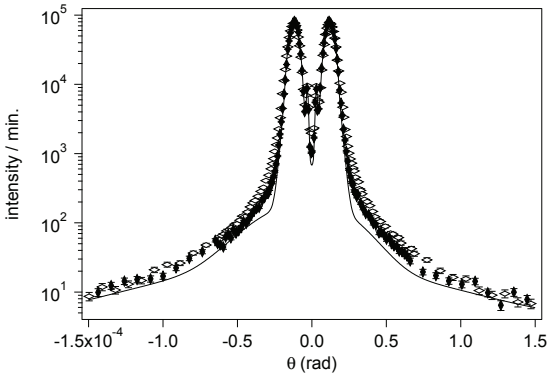

Figure 3. Diffraction patterns obtained with $B = 0\,\mathrm{G}$ for vertical (♦) and horizontal (◊) orientation of the amorphous sample ribbon. The full line represents the rocking curve.

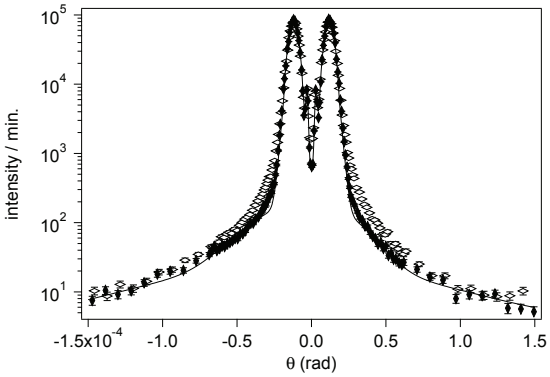

Figure 4. Analogous intensity distributions measured when this extremely soft-magnetic sample is magnetically saturated at $B = 10.9\,\mathrm{G}$.

orientation of the ribbon, the ribbon possesses a transverse magnetic texture, indeed.

On the other hand, Fig. 5 shows that a significant reduction of scattered intensity for the vertically aligned ribbon upon applying a longitudinal external tensile stress of 82 MPa, well above the (∼50 MPa) which were applied during the texture-forming thermal treatment of the sample. This means that because of the positive sign of the magnetostriction constant the transverse magnetic texture vanishes or may even be transformed into a longitudinal one. However, to unambiguously verify such a transformation a comparison with the results of an additional measurement with horizontally aligned ribbon under under external stress would be required.

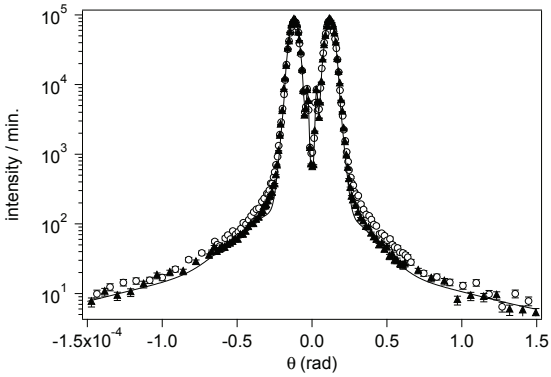

Figure 5. Influence of an externally applied tensile stress on the measured intensity distributions for vertical orientation of the sample ribbon: (○) $\sigma = 0\,\mathrm{Mpa}$, (▲) $\sigma = 82\,\mathrm{MPa}$. Again, the full line represents the rocking curve obtained without sample, i.e. the instrumental resolution function.

As mentioned already in the introduction, scattering from this sample ribbon is generally quite low and partly hidden behind the instrumental resolution function. Therefore we did not aim on a detailed determination of the shape of the magnetic inhomogeneities, which would require better statistics at the wings, but just tried to extract reasonable information about their overall size. We started by subtracting an arbitrary percentage $R(\theta) \times (1 - P_{\mathrm{scat}})$ of the rocking curve $R(\theta)$ from the measured raw data, where P_{scat} denotes the scattering probability. Subsequently a least square fit to the shoulders of the resulting 'pure' scattering distribution was performed according to a Guinier approximation of the form $I(\theta) \propto \exp(-kL \sin\theta)^2$, with L as fit parameter and θ the scattering angle. (The proportionality factor is governed by the number of scatterers, and the squares of their volumes and mean scattering length density differences.)

For each of the measured raw intensity distributions this procedure was repeated about 10^3 times with different values of $P_{\rm scat}$ and L. From the fit yielding the smallest χ^2 we inferred both the most likely scattering probability, typically $P_{\rm scat}$ of the order 10–20%, and the size parameter L. Assuming domains of approximately rectangular cross-section, the horizontal dimension of the mean effective rectangle is then given by $a = L\sqrt{12}$. Fig. 6 and Fig. 7 illustrate the results of this procedure for the field dependence of the scattered intensity with vertically aligned ribbon.

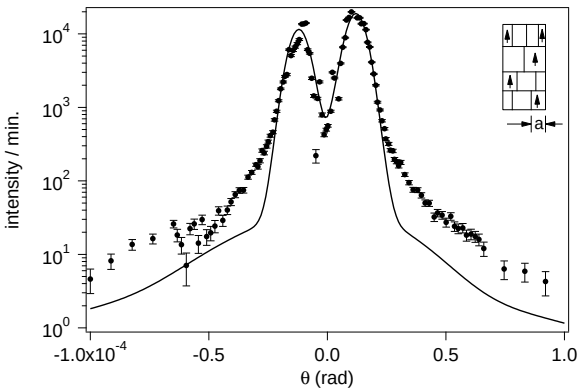

Figure 6. 'Pure' scattered intensity for vertically oriented ribbon (●) at $B = 0\,\mathrm{G}$ and $\sigma = 0\,\mathrm{MPa}$ after subtraction of the most likely non-scattered contribution. The solid line corresponds to a Guinier fit to the peaks of this intensity distribution, convolved with the measured resolution function of Fig. 2 (for details of the underlying procedure see the text).

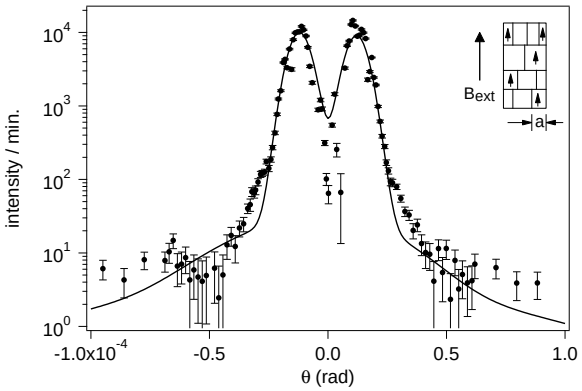

Figure 7. The analogous distribution (●) obtained at $B = 10.9\,\mathrm{G}$ and $\sigma = 0\,\mathrm{MPa}$ and the corresponding Guinier fit to the peaks (——), again convolved with the resolution curve. The inset illustrates the orientation of the ribbon and the applied magnetic field as well as the meaning of the size parameter a.)

The influence of an externally applied tensile stress on the scattered intensity distribution is seen from a comparison of Figs. 6 and 8.

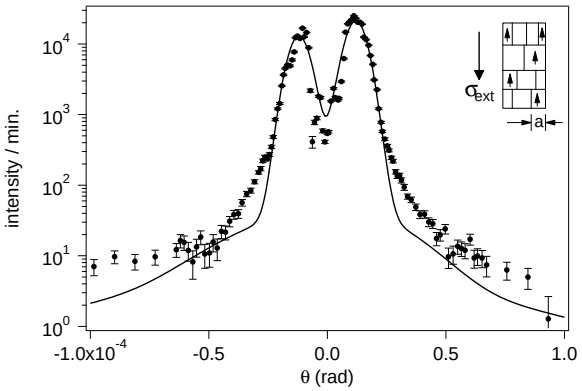

Figure 8. The 'pure' scattered intensity distribution (●) measured at $B = 0\,\mathrm{G}$ when an external tensile stress $\sigma = 82\,\mathrm{MPa}$ is applied to the ribbon, which is appreciably larger than the stress of 50 MPa which was applied during the fabrication process of the ribbon in order to induce a transverse magnetic anisotropy. The meaning of the inset is analogous to that of the previous figures.

Finally, in Fig. 9 the field and the stress dependence of the size parameter a is shown. It shall be noticed that the statistical errors are about as large as the symbols. Systematic errors of the absolute values of the size of the magnetic inhomogeneities are difficult to estimate, however. But the overall tendency upon variation of field and tensile stress seems to be quite reliable. At

a very small external field the transverse magnetic texture of the ribbon is obviously removed and the magnetic domains have roughly the same size in vertical and horizontal direction. With increasing field the size of the now vertically aligned domains starts to increase as well (naturally on the cost of their number). In the case of horizontal ribbon alignment, where the field is orthogonal to the ribbon axis, the size of the transversely oriented domains is slightly decreasing with increasing field. It is interesting to see that an increasing external tensile stress along the ribbon axis leads to a similar behavior than that obtained by applying a magnetic field. Up to a tensile stress of $\sigma \sim 60$ MPa the size of the transverse domains is decreasing. Above this value, which is in good agreement with the expected limit due to the thermal treatment, the stress-induced transverse magnetic anisotropy is completely overcome and growing of the domains - now aligned along the ribbon axis because of positive magnetostriction - starts again.

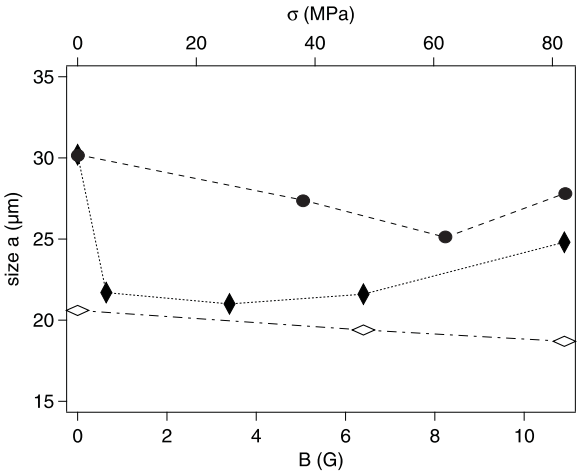

Figure 9. Field dependence of the domain size parameter a (see inset of Fig. 6) for vertical (⧫) and horizontal (◊) orientation of the sample ribbon. Furthermore the variation of a with increasing externally applied tensile stress is shown for vertical ribbon orientation in the absence of any magnetic field (•). The statistical errors correspond roughly to the sizes of the symbols.

4. Concluding comment

It is clear that the USANSPOL technique came close or even went beyond its limits upon encountering the very large magnetic domains of this specific soft-magnetic amorphous ribbon, which turned out to be of the order of 20-30 μm. But it is remarkable that nevertheless it could provide valuable information about the internal magnetic structure of the sample. Although the scattering probabilities are relatively large compared to a typical SANS experiment, we did not need to concern ourselves with multiple neutron scattering since on their passage through the ribbon the neutrons encounter a single scatterer and its surroundings only. This is concluded from the fact that the thickness of the ribbon of $\sim$25 μm also corresponds to the domain sizes determined by our measurements.

Acknowledgments

The authors wish to thank H. Lemmel and R. Loidl for their invaluable support. This project was supported by Hochschuljubiläumsstiftung der Stadt Wien (Proj. No. H-1851/2006).

References

[1] Littrell K and Lee W 2004 *Physica* B **345** 246
[2] Wagh A G, Rakhecha V, Strobl M and Treimer W 2004 *Pramana J. Phys.* **63** 369
[3] Jericha E, Badurek G and Trinker M 2007 *Physica* B **397** 88
[4] Jericha E, Baron M, Hainbuchner M, Loidl R, Villa M and Rauch H 2003 *J. Appl. Cryst.* **36** 778
[5] Badurek G, Buchelt R J, Kroupa G, Baron M and Villa M 2000 *Physica* B **283** 389